Born-Oppenheimer surface of triatomic silicon and its relationship to potentials in the bulk

P. Dallot* and P. D. Bristowe
Department of Materials Science and Engineering, Massachusetts Institute of Technology, Cambridge, Massachusetts 02139
(Received 23 August 1991)

The Born-Oppenheimer (BO) surface of triatomic silicon is investigated and accurately described using two- and three-body potentials. The topology of the BO surface is found to be unstable with respect to fluctuations in these potentials, indicating that it is nongeneric. Examination of the two- and three-body components shows that the topology of the three-body term is fundamentally different from that of potentials usually used to model crystalline silicon. A study was therefore made to determine under what conditions this topology could successfully reproduce the diamond cubic structure of crystalline silicon. Two limiting methods for applying these potentials in the bulk have been considered and appraised. One of them uses the *exact* two- and three-body terms, and approximates the effect of the remaining terms in the N-body expansion (the screening effect) with a four-body term. The other method consists of screening the two- and three-body terms directly. Both methods were unsuccessful in reproducing the diamond cubic structure, which indicates the importance of terms of order higher than 4.

I. INTRODUCTION

Extensive technological interest in the elemental semiconductor silicon has resulted in many fundamental studies of a theoretical nature aimed at understanding the basic interatomic forces that bond this important covalent material. Both quantum-mechanical and classical approaches have been employed to study silicon in either its bulk state[1-3] or in the form of small atomic clusters.[4-6] Atomic and electronic structures have been predicted based on interatomic potentials that are either derived or assumed. Of interest have been the nucleation and growth of clusters into the bulk crystalline or amorphous phase and of the properties of various defects that affect the electronic characteristics of the crystalline material.

All the calculations begin with a description of the many-body interactions existing in the solid. The present study is motivated by an interest in understanding how the shape of an interatomic potential, used, for example, in an atomistic calculation, influences the physical properties of the crystal it models. In particular, the investigation focuses on the question of whether the exact first terms in the N-body expansion of the potential are structure determining or not. Accurate approximations to the two- and three-body terms of this expansion are therefore computed, which together form the only existing model for the Born-Oppenheimer surface of triatomic silicon. The computational method employed and the topological analysis of the results (the Born-Oppenheimer surface of triatomic silicon is found to be nongeneric) are described in Sec. II. For the construction of the three-body potential, a reduced coordinate scheme is used, which is described in a companion paper.[7] Section III describes two approaches used to adjust these potentials to reproduce the bulk properties of silicon. One approach uses the exact two- and three-body terms that are computed and attempts to account for the remaining terms that are neglected through a four-body term. Another approach employs only rescaled two- and three-body terms which retain, however, their original topology. Neither of these two limiting methods produced entirely satisfactory results, which indicated that terms of order higher than 4 in the N-body expansion are important.

II. THE BORN-OPPENHEIMER SURFACE OF DIATOMIC AND TRIATOMIC SILICON

The construction of the exact two- and three-body potentials for silicon relies on combining first-principles calculations with an analysis of the configuration space of two and three atoms. To calculate accurate configurational energies, the total-energy pseudopotential approach[8] is employed, which, for silicon, provides an excellent approximation to the interatomic interactions of interest. The geometrical analysis of two and three-atom clusters provides a way of selecting certain symmetry configurations that will dictate the form of the potential.

The two- and three-body potentials differ widely in this latter respect. Since the geometry of two atoms is determined by their interatomic distance, the value of the energies for a collection of interatomic distances (about ten of them) is all that is required to obtain an idea of the form of the two-body potential. The use of a similar grid in the three-body configuration space would prove intractable since it would require an order of 10^3 calculations. Instead, a procedure is used which relies on the properties of subspaces of high symmetry present in that configuration space. It is known that saddle points are bound to be present on these subspaces from the principle of symmetry-dictated extrema. Anticipating the topology of the three-body term to be relatively simple (on physical grounds), it is supposed that all the saddle points are located on these subspaces. Each saddle point is then examined in a systematic way. It is subsequently verified, using general topological principles (in practice, by in-

spection, given the relatively small number of distinct forms), that the local behavior of the potential around each saddle point are consistent with one another. The result that is obtained is surprising in that the topology of the three-body terms turns out to be one of the simplest possible, involving no more than three different critical points (one minimum, one maximum, and one saddle point).

Sections II A–II D describe the pseudopotential calculations, the method used to account for spin polarization, the total energies or two- and three-atom clusters, and the use of these results in the construction of two- and three-body potentials.

A. Pseudopotential method and treatment of spin polarization

The total energy of the various atomic configurations involving two or three atoms were computed using a total-energy program developed by Payne *et al.*,[9] which uses a scheme of convergence based on the Car and Parrinello method.[10] In this method ionic motion and electronic relaxations are treated simultaneously during the computation of low-energy structures. However, in the present study it is the energy of a series of specific ionic structures that is of interest and therefore only electronic relaxation was allowed. The approximations used to calculate the total energy of the clusters are the local-density approximation (LDA) within density-functional theory,[11] the pseudopotential approximations,[12] the use of supercells, a finite basis set, and a finite number of **k** points to perform Brillouin-zone averaging.

The Hamann-Schlüter-Chiang (HSC) pseudopotential[12] for silicon was used with a kinetic-energy cutoff at 10 Ry and only one special **k** point was considered: (0,0,0). The size of the computational cell was such that the motif composed of clusters of two or three atoms did not interact with its periodic images. A computation of the electron density on the walls of the simulation cell provided a way of verifying that these image interactions were small.

An important drawback in the above approach is that it does not take into account electron spin. It is well known that when degeneracies appear near the valence level, the electrons first occupy the various degenerate orbitals with parallel spins so as to minimize their exchange energy. In the following discussion this effect is analyzed qualitatively for the case of the isolated silicon atom and the diatomic molecule. Previous results obtained elsewhere[4–6] for the triatomic molecule are also summarized. It is concluded that the spin-polarization effect is important for the isolated atom and diatomic molecule, but relatively small for triatomic molecules. Consequently, a procedure for modifying the results of the pseudopotential calculations is proposed.

Isolated atom. The atomic number of silicon is 14, so that the $3p$ orbitals are populated by two electrons. To be consistent with the molecules treated below, the two orbitals p_x and p_y are called α_a and β_a. As the energy of these states is different from that of the other levels and does not mix with them, they are treated independently in a Hartree-Fock formalism.

The spatial part of the two-electron wave function is equal to

$$|\Psi_\varepsilon\rangle=\frac{1}{\sqrt{2}}[|\alpha_a(1),\beta_a(2)\rangle+\varepsilon|\alpha_a(2),\beta_a(1)\rangle] , \quad (1)$$

where $\varepsilon=+1$ corresponds to the antisymmetric state of spin and $\varepsilon=-1$ is the symmetric state of spin. A simple derivation shows that the average electron-electron interaction energy is equal to

$$\langle\Psi_\varepsilon|V_{12}|\Psi_\varepsilon\rangle=U+\varepsilon I , \quad (2)$$

where U and I are the Coulomb and exchange integrals, respectively, given by

$$U=\langle\alpha_a(1),\beta_a(2)|V_{12}|\alpha_a(1),\beta_a(2)\rangle , \quad (3)$$

$$I=\langle\alpha_a(1),\beta_a(2)|V_{12}|\alpha_a(2),\beta_a(1)\rangle . \quad (4)$$

The exchange energy per atom is therefore equal to $2I$.

Diatomic molecule. The valence configuration of diatomic silicon at equilibrium is

$$\ldots 3s\sigma_g^2 3s\sigma_u^{*2} 3p\sigma_g^2 3p\pi_u^2 .$$

It therefore exhibits two degenerate π states populated by only two electrons. To a first approximation, the analysis above applies. The corresponding one-electron states are approximately

$$|\alpha\rangle=\frac{1}{\sqrt{2}}[|\alpha_a(1)\rangle+|\alpha_b(1)\rangle] , \quad (5)$$

$$|\beta\rangle=\frac{1}{\sqrt{2}}[|\beta_a(1)\rangle+|\beta_b(1)\rangle] , \quad (6)$$

where α_a and β_a represent the p_x and p_y orbitals of atom a, and α_b and β_b represent the p_x and p_y orbitals of atom b. The exchange energy is then equal to

$$2I'=2\langle\alpha(1),\beta(2)|V_{12}|\alpha(2),\beta(1)\rangle , \quad (7)$$

which can be represented as

$$\begin{aligned}2I'=\tfrac{1}{2}[&\langle\alpha_a(1),\beta_a(2)|V_{12}|\alpha_a(2),\beta_a(1)\rangle\\&+\langle\alpha_b(1),\beta_b(2)|V_{12}|\alpha_b(2),\beta_b(1)\rangle]\\&+\text{two center integrals} .\end{aligned} \quad (8)$$

Neglecting the two-center integral terms yields an exchange energy equal to

$$2I'=I . \quad (9)$$

It is one-fourth of the exchange energy for two isolated atoms. It is not small, and should be taken into account when fitting the two-body potential.

For small interatomic distances, the electronic configuration becomes that of carbon, which is $\ldots 3s\sigma_g^2 3s\sigma_u^{*2} 3p\pi_u^4$ (the $3p\sigma_g$ state and the $3p\pi_u$ states switch their order), so that all valence levels are fully occupied. The spin-polarization effect is therefore equal to zero in that case. Hence, the curve of spin-polarization effect versus interatomic distance (which we refer to as the spl curve) is expected to go smoothly from zero (short distances) to $4I$ (large distances), with an intermediate

value of I at the equilibrium distance. The curvature of the spl curve should therefore be small at the equilibrium distance so that the energy values given by the pseudopotential calculations accurately reproduce the vibration frequencies. The slope of the spl curve should result in a displacement of the equilibrium distance, but this effect is small since the curvature is large at this location. The main effect of spin polarization appears to be a modification of the long-range interaction behavior which is taken into account by truncating the computed energies so as to restore the cohesive energy of diatomic silicon.

Triatomic molecules. A generic configuration with no particular symmetry will have nondegenerate energy levels. Its spin-polarization energy will therefore be significant only in the region of configuration space where atoms are far enough from each other to be considered isolated. In this case, the approximation which truncates the computed energies so that they do not exceed the reference energy of three isolated atoms seems fully justified (only the spin-polarization energy of isolated atoms is taken into account). The only approximation involved occurs far away from the region where the energy is low and therefore far away from the region of interest. The problem is more complicated for symmetric configurations.

Symmetric configurations of triatomic silicon have been studied extensively.[4–6] Reproduced here are some of the previously published results from which it can be concluded that the spin-polarization energy is equal to zero over a neighborhood of the critical points of the Born-Oppenheimer surface. The configurations of symmetry considered are the linear configuration (group $D_{\infty h}$), the isosceles triangle (group C_{2v}), and the equilateral triangle (group (D_{3h}).

The previous studies[4–6] report the following electronic structures for the valence levels:

$$D_{\infty h} \quad \ldots 2\sigma_u^2 1\pi_u^4 ,$$

$$C_{2v} \quad \ldots 3a_1^2 1b_1^2 ,$$

$$D_{3h} \quad \ldots 1a_2''^2 e'^4 .$$

Here, the states corresponding to σ, a_1, b_1, a_2'' belong to one-dimensional representations and can be occupied by no more than two electrons. The states corresponding to π and e' belong to two-dimensional representations and are filled with four electrons. There is no partially occupied level, so that the spin-polarization effect is equal to zero for all of these configurations.

The same procedure is then applied to symmetry configurations as was introduced for generic configurations. The computed energies are truncated in the region where atoms are far away from each other so that the total energy does not exceed the energy of three isolated atoms.

B. Total energies for two- and three-atom clusters

The two-body calculations were performed in a cube with side equal to 9.2 Å with the two atoms aligned along the main diagonal. Since the cutoff energy was equal to 10 Ry, it defined a sphere containing 1989 plane waves used to span reciprocal space. Only one special **k** point was used: (0,0,0), and the first four electronic levels were filled with two electrons each. The spin-polarization energy was taken into account through a truncation of the computed energies. It was estimated to be equal to 0.75 eV for the isolated atom. The results are summarized in Table I.

The three-body calculations were performed in a rectangular box with dimensions $15\times15\times8$ Å^3. The three atoms were located in the (0,0,1) plane. Since the cutoff energy was still be equal to 10 Ry, it now defined a sphere containing 6503 plane waves used to span reciprocal space. Again, only one special **k** point was used: (0,0,0), and the first six electronic levels were each filled with two electrons. The energies of configurations surrounding each saddle point were calculated. The configurations were indexed by their reduced coordinates:[7]

$$(\rho, \sin^2(3\theta/2), \sin(2\varphi)) .$$

where ρ is a radius in the three-body configuration space and the two other coordinates define the geometry of the configuration. This coordinate system is described in more detail in a companion paper.[7] The energies corresponding to geometries surrounding those of the different saddle points, for different radii, were therefore computed. The spin-polarization energy was taken into account through a truncation of the computed energies. It was estimated to be equal to 0.75 eV for the isolated atom. These results are summarized in the first two columns of Tables II–V.

C. Choosing a functional form for the two- and three-body potential

To construct the two-body potential, a function is required which reproduces the computed total-energy data as closely as possible. However, uncertainty in the estimated spin-polarization energy (SPE) created a large set

TABLE I. Computed two-body energies.

Interatomic distance (Å)	Total energy (eV)	Including spin polarization and atomic energy (eV)
1.352	−194.7694	10.683
1.577	−203.9289	1.5233
1.803	−207.3952	−1.9430
1.915	−208.0196	−2.5674
2.028	−208.3020	−2.8498
2.141	−208.3715	−2.9194
2.253	−208.4260	−2.9738
2.480	−208.2043	−2.7521
2.704	−207.7306	−2.2785
3.155	−206.5825	−1.1303
3.606	−205.5915	−0.1393
4.056	−204.84	0.0
4.507	−204.25	0.0
4.958	−204.08	0.0
5.408	−203.95	0.0
5.634	−203.93	0.0

TABLE II. Equilateral triangles $(r,0,0)$. Geometry of the first saddle point.

Reduced coordinates	Total energy (eV)	Including spin polarization (eV)	Minus two-body term and atomic energy
(3,0,0)	−307.8612	−307.8612	3.2487
(4,0,0)	−314.7442	−314.7442	1.4945
(5,0,0)	−315.9692	−315.9692	0.2999
(6,0,0)	−315.5578	−315.5578	−0.3560
(9,0,0)	−312.6777	−312.6777	−0.6007
(13,0,0)	−309.7837	−309.7837	−0.0703
(20,0,0)	−307.0580	−307.45	0.0
(30,0,0)	−305.7014	−307.45	0.0

of functions from which to choose. The choice of a functional form for the two-body term was actually guided by the need to find a functional form for the three-body term. A major requirement for this choice is that the energy differences between the three-body energy (as given by the pseudopotential calculations) and the two-body contribution be small and smoothly varying. This requirement enabled various two-body terms to be selected as well as providing a choice of different methods to account for the SPE.

The final choice of functional form was a Morse potential and it was found necessary to account for the SPE using the same procedure used for the three-body term. Specifically, the computed energies were truncated at a value equal to the computed energy for a large interatomic distance minus twice the atomic SPE (equal to 0.75 eV). The SPE at the equilibrium distance was therefore disregarded, so that the two-body potential obtained is relatively inaccurate. The cohesive energy it yields is too low by 0.2 eV and the vibration frequency at equilibrium is too small by a factor of 2. This proved to be the only procedure considered that enabled a smooth three-body term to be constructed. It was chosen as a compromise between the need to reproduce diatomic properties and

TABLE III. Linear geometry $(r,0,1)$. Geometry of the second saddle point.

Reduced coordinates	Total energy (eV)	Including spin polarization (eV)	Minus two-body term and atomic energy
(8,0,1)	−308.3076	−308.3076	1.1520
(10,0,1)	−313.7810	−313.7810	−0.6922
(13,0,1)	−315.5952	−315.5952	−1.8225
(20,0,1)	−313.4613	−313.4613	−1.6296
(30,0,1)	−309.8668	−309.8668	−0.0976
(50,0,1)	−306.7667	−307.45	0.0
(80,0,1)	−305.4709	−307.45	0.0
(8,0,0.99)	−313.6574	−313.6574	−0.5233
(10,0,0.99)	−315.6742	−315.6742	−1.5804
(13,0,0.99)	−315.2464	−315.2464	−1.9969
(8,0.01,1)	−307.4299	−307.4299	1.2801
(10,0.01,1)	−313.2381	−313.2381	−0.6021
(13,0.01,1)	−315.3468	−315.3468	−1.7465
(10,0.01,0.99)	−315.4917	−315.4917	−1.5336
(10,0.01,0.99)	−315.1765	−315.1765	−1.9576
(6,0,0.946)	−312.3486	−312.3486	0.1751
(8,0,0.946)	−315.8504	−315.8504	−1.3626
(10,0,0.946)	−315.7248	−315.7248	−1.8970
(14,0,0.946)	−313.4796	−313.4796	−1.6465
(20,0,0.946)	−310.4338	−310.4338	−0.5549
(30,0,0.946)	−307.7213	−307.7213	0.0
(50,0,0.946)	−305.8230	−307.45	0.0
(5,0,0.9)	−310.3895	−310.3895	1.0133
(6,0,0.9)	−314.4295	−314.4295	−0.3340
(8,0,0.9)	−316.1203	−316.1203	−1.5748
(10,0,0.9)	−315.2996	−315.2996	−1.8823
(14,0,0.9)	−312.6691	−312.6691	−1.3837
(20,0,09)	−309.7028	−309.7028	−0.2710

TABLE IV. Geometry of the equilibrium position (6.125,0,0.666).

Reduced coordinates	Total energy (eV)	Including spin polarization (eV)	Minus two-body term and atomic energy
(4,0,0.666)	−311.4111	−311.4111	1.5478
(5,0,0.666)	−315.4131	−315.4131	0.0141
(6.125,0.0.666)	−316.3046	−316.3046	−0.9545
(7,0,0.666)	−316.0342	−316.0342	−1.3517
(12,0,0.666)	−312.0214	−312.0214	−1.0435
(20,0,0.666)	−308.1916	−308.1916	0.0
(40,0,0.666)	−305.6584	−307.45	0.0
(5,0.02,0.666)	−315.3678	−315.3678	0.0273
(6.125,0.02,0.666)	−316.2760	−316.2760	−0.9414
(7,0.02,0,666)	−316.0124	−316.0124	−1.3379
(5,0,0.6)	−315.7424	−315.7424	−0.0264
(6.125,0,0.6)	−316.2782	−316.2782	−0.9461
(7,0,0.6)	−315.8650	−315.8650	−1.3038
(5,0.1,0.666)	−315.2540	−315.2540	0.0118
(6.125,0.1,0.666)	−316.1616	−316.1616	−0.8899
(7,0.1,0.666)	−315.9077	−315.9077	−1.2654
(5,0,0.6)	−315.1650	−315.1650	0.0528
(6.125,0,0.6)	−316.2890	−316.2890	−0.9459
(7,0,0.6)	−315.9890	−315.9890	−1.2431

the need to construct a three-body term.

Another way of viewing the relationship between two- and three-body terms is to think of the three-body term as partly screening in the two-body term. Consider the Morse form that was used:

$$V_2(r)=A\exp^{(-\alpha r^2)}+B\exp^{(-\beta r^2)}\ . \tag{10}$$

Is it possible to approximate the two-body contribution it gives for a system of three atoms by a pure three-body term? Since the interatomic distances and the reduced coordinates[7] have the following relationship:

$$\begin{aligned} r_{12}^2&=\rho[\cos\varphi+\sin\varphi\cos\theta]\ ,\\ r_{13}^2&=\rho[\cos\varphi-\sin\varphi\cos(\pi/3-\theta)]\ ,\\ r_{23}^2&=\rho[\cos\varphi-\sin\varphi\cos(\pi/3+\theta)]\ , \end{aligned} \tag{11}$$

the two-body term contribution to the total energy of three atoms is obtained as

$$\begin{aligned} \sum V_2(r)=&A\exp[-\alpha\cos(\varphi)\rho]\{\exp[-\alpha\sin(\varphi)\cos(\theta)\rho]+\exp[\alpha\sin(\varphi)\cos(\pi/3-\theta)\rho]+\exp[\alpha\sin(\varphi)\cos(\pi/3+\theta)\rho]\}\\ &+B\exp[-\beta\cos(\varphi)\rho]\{\exp[-\beta\sin(\varphi)\cos(\theta)\rho]+\exp[\beta\sin(\varphi)\cos(\pi/3-\theta)\rho]+\exp[\beta\sin(\varphi)\cos(\pi/3+\theta)\rho]\}\ . \end{aligned} \tag{12}$$

TABLE V. Additional data, related to oher regions of the configuration space.

Reduced coordinates	Total energy (eV)	Including spin polarization (eV)	Minus two-body term and atomic energy
(4,0.5,0.666)	−309.6575	−309.6575	1.9431
(6.125,0.5,0.666)	−315.5473	−315.5473	−0.6052
(8,0.5,0.666)	−314.9607	−314.9607	−1.2492
(12,0.5,0.666)	−312.0096	−312.0096	−0.9770
(20,0.5,0.666)	−308.3068	−308.3068	−0.3295
(30,0.5,0.666)	−306.3154	−307.45	0.0
(60,0.5,0.666)	−305.2155	−307.45	0.0
(4,1,0.666)	−307.7806	−307.7806	2.4236
(6.125,1,0.666)	−314.5756	−314.5756	−0.0809
(8,1,0.666)	−314.3587	−314.3587	−0.7542
(12,1,0.666)	−311.3587	−311.3587	−0.8588
(20,1,0.666)	−308.3980	−308.3980	−0.3169
(30,1,0.666)	−306.4473	−307.45	0.0
(60,1,0.666)	−305.2412	−307.45	0.0

It is therefore not possible, in general, to express the two-body contribution along a direction (defined by θ and φ) as a Morse form in terms of $(\rho)^{1/2}$ (with coefficients depending upon θ and φ). It is expected, however, that as ρ increases, one of the three exponential terms appearing in each of the summation factors to A or B will become dominant so that a Morse form would correctly approximate the two-body contribution along such a direction. This, indeed, was found to be the case with surprising accuracy. However, this form was not successful in reproducing the three-body energies summarized in the last column of Tables II–V. Instead, a Morse form in terms of ρ was used [instead of $(\rho)^{1/2}$] which then yielded very good results. Further consideration of the morphology of the three-body potential led to a three-body term with the form

$$V_3(\rho,s_1,s_2)=t(s_1)g(s_2,\rho)+[1-t(s_1)]g(-s_2,\rho)\ , \quad (13)$$

with

$$g(s_2,\rho)=A(s_2)\exp[-\alpha(s_2)\rho^2]+B(s_2)\exp[-\beta(s_2)\rho^2]\ , \quad (14)$$

where

$$(s_1,s_2)=(\sin^2(3\theta/2),\sin(2\varphi))$$

and A,α,B,β are polynomials in s_2. t is a monotonic function taking values between zero and 1 such that $t(0)=1$ and $t(1)=0$.

To conclude this section, it is emphasized that there exists an important dependency between the functional forms of the two- and three-body terms. It is this dependency that guides the choice of both functional forms. The results obtained can be summarized with two points. First, the spin-polarization effect was accounted for in a unified way for both the two- and the three-body energies. Second, it was found that the Morse form gave good results for both the two- and the three-body term, but involved different forms of exponential decay. The two-body term decreases as $\exp(-\alpha r^2)$, where r is the interatomic distance. The three-body term decreases as $\exp(-\alpha\rho^2)$, where ρ is the radius in the three-body configuration space and varies as r^2.

D. Fitting the functional forms to the total energies

For the two-body potential, a conjugate gradient method is used to optimize the data given in Table I. The following values for the coefficients of the Morse form [see Eq. (10)] are then obtained:

$$A=194.867\,096\,642\,77\ ,$$

$$\alpha=1.359\,991\,465\,251\,6\ ,$$

$$B=-7.722\,190\,281\,325\,6\ ,$$

$$\beta=0.178\,909\,578\,526\,89\ .$$

These coefficients yield the two-body energies that are summarized in Table VI (second column). The equilibrium distance is found to be 2.11 Å [expected value 2.23 Å (Ref. 13)] and the minimum energy is given as -3.01 eV [expected value -3.21 eV (Ref. 13)]. The curvature of the potential at the energy minimum is equal to 6.21 eV/Å^2, compared to 13.45 eV/Å^2 for the experimental value.[13]

Consider now the three-body potential. Tables II–V indicate the existence of four critical points on the Born-Oppenheimer surface of triatomic silicon. These saddle points are (i) a global minimum in an obtuse isosceles configuration, (ii) a first saddle point (degenerate, due to symmetry) in an equilateral configuration, (iii) a second saddle point (in order of increasing energy) in a linear isosceles configuration, and (iv) a global maximum at the origin.

It is assumed, as the data strongly suggest, that these saddle points are the only ones. This assumption was the final guideline used in deciding the functional form of the three-body term. Examination of this form given in Eq. (13) shows that the function g represents the V_3 values

TABLE VI. Two-body potential energies.

Interatomic distance (Å)	Computed energies (eV)	Reference energies from Table I (eV)
1.352	10.6473	10.683
1.577	1.6592	1.5233
1.803	−1.9726	−1.9430
1.915	−2.6792	−2.5674
2.028	−2.9746	−2.8498
2.141	−3.0186	−2.9194
2.253	−2.9177	−2.9738
2.480	−2.5264	−2.7521
2.704	−2.0777	−2.2785
3.155	−1.3009	−1.1303
3.606	−0.7544	−0.1393
4.056	−0.4067	0.0
4.507	−0.2039	0.0
4.958	−0.0950	0.0
5.408	−0.0412	0.0
4.634	−0.0264	0.0

for the isosceles triangles ($s_1=0$ or 1). The obtuse configurations of isosceles triangles (among which is the energy minimum) are such that $s_1=0$ and then V_3 will be equal to the values of g taken on positive values of the first variable ($+s_2$). The other isosceles configurations (acute) are such that $s_1=1$ and then V_3 will be equal to the values of g taken on negative values of the first variable ($-s_2$). The coordinate s_1 allows a nonsymmetric configuration to be viewed as an intermediate state between two isosceles configurations, one being obtuse and the other acute. The three-body energy is then interpolated between these two points using the coefficients t and $1-t$. Hence, it is seen that if g is chosen such that

$$g(s_2,\rho)<g(-s_2,\rho) \text{ for all } (s_2,\rho)\in\mathbb{R}^+\times\mathbb{R} , \quad (15)$$

then the monotonic nature of t implies that the critical points (extrema and saddle points) of the potential will all be isosceles triangles as intended.

Among the various saddle points, special attention should be given to the equilateral configuration, since its highly symmetric structure makes it likely to be degenerate. Intuitively, it is expected that the total energy will increase during deformation of the structure from the equilateral saddle point towards an acute isosceles configuration and then to decrease again as the structure is deformed into an obtuse isosceles configuration. This behavior would imply that the second derivative of the total energy with respect to s_2 is equal to zero and consequently the local behavior is controlled by the third-order term. The equilateral saddle point would then be degenerate (the local shape would not be entirely controlled by the second differential), and appear as an inflection point on the curve of energy versus s_2 (at constant ρ in the plane of isosceles triangles).

Upon consideration of the two-body contribution to the total energy [Eq. (12)], it can be seen that its second derivative with respect to s_2, which is equal to

$$\frac{\partial^2\sum V_2}{\partial s_2^2}(s_2=0)=\alpha\rho(\alpha\rho+3)A\exp(-\alpha\rho)+\beta\rho(\beta\rho+3)B\exp(-\beta\rho) \quad (16)$$

when $s_2=0$, is different from zero everywhere except on a finite set of points along the line of equilateral triangles. The second differential of the two-body contribution is therefore generally nondegenerate. The three-body term that is added to obtain the total energy has to cancel exactly this behavior, since otherwise the equilateral saddle point will not be degenerate and will correspond to either a local minimum (undercompensation of the two-body energy) or to a saddle point between two local minima in the plane of isosceles triangles (overcompensation of the two-body energy).

Since exact compensation is difficult to obtain, two types of three-body potential have been constructed which illustrate both types of behavior. The first of these potentials (potential α) gives a good fit to the computed data and illustrates the situation of overcompensation. It was developed using the functional form given in Eq. (13) and the following expressions for A, α, B, β, and t:

$$\begin{aligned} A&=a_0+(s_2)^3\left[a_3+a_4\left[\frac{1.1+s_2}{2.1}\right]^{a_5}\right] ,\\ \alpha&=\alpha_0+\alpha_2(s_2)^2+\alpha_3(s_2)^3+\alpha_4(s_2)^4 ,\\ B&=b_0+b_2(s_2)^2+b_3(s_2)^3+b_4(s_2)^4 ,\\ \beta&=\beta_0+\beta_2(s_2)^2+\beta_3(s_2)^3+\beta_4(s_2)^4 ,\\ t&=1-s_1\tau_1-s_1^2\tau_2-s_1^3(1-\tau_1-\tau_2) . \end{aligned} \quad (17)$$

The numerical values of the various coefficients in these expressions are given in Table VII.

The second of these potentials (potential β) gives a slightly poorer fit to the computed data and illustrates the situation of undercompensation. Since the secondary derivative of the two-body contribution with respect to s_2 is small, a three-body term is chosen which also has a zero secondary derivative with respect to s_2. This condition was obtained with the following forms for A, α, B, β, and t:

$$\begin{aligned} A&=a_0+(s_2)^3\left[a_3+a_4\left[\frac{1.1+s_2}{2.1}\right]^{a_5}\right] ,\\ \alpha&=\alpha_0+\alpha_3(s_2)^3+\alpha_4(s_2)^5 ,\\ B&=b_0+b_3(s_2)^3+b_4(s_2)^4+b_5(s_2)^5 ,\\ \beta&=\beta_0+\beta_3(s_2)^3+\beta_4(s_2)^4+\beta_5(s_2)^5 ,\\ t&=1-s_1\tau_1-s_1^2\tau_2-s_1^3(t-\tau_1-\tau_2) , \end{aligned} \quad (18)$$

where the various fitted coefficients are given in Table VIII.

The main difference between these two potentials concerns their local morphology around the equilateral saddle point. This difference is shown schematically in Fig. 1, which represents the location of the saddle points in three-body configuration space. Figure 1(a) shows the location of the equilateral saddle point (E) in the three-body configuration space. Figures 1(b)–1(d) represent slices with $z=$const through the three-body configuration space that include the saddle point E. Arrows indicate the directions of the energy gradients. Figure 1(b) represents the expected shape of the Born-Oppenheimer surface around the saddle point E. Figure 1(c) represents the situation of overcompensation (potential α), and Fig. 1(d) represents that of undercompensation (potential β). Each figure shows the existence of sad-

TABLE VII. Fitted coefficients for potential α.

$a_0=9.274\,009\,096\,770\,5$	$a_0=6.526\,187\,043\,519\,8\times10^{-2}$
$a_3=0.229\,263\,361\,116\,33$	$a_2=-1.444\,894\,119\,065\,7\times10^{-2}$
$a_4=5.962\,675\,583\,054\,5$	$a_3=4.241\,528\,351\,458\,6\times10^{-3}$
$a_5=403$	$a_4=-3.594\,439\,060\,800\,4\times10^{-2}$
$b_0=-2.040\,650\,939\,475\,2$	$b_0=1.195\,906\,845\,501\,3\times10^{-2}$
$b_2=-2.042\,714\,932\,644\,4$	$b_2=-5.483\,188\,734\,850\,3\times10^{-3}$
$b_3=-1.972\,202\,404\,850\,3$	$b_3=1.371\,158\,806\,739\,0\times10^{-3}$
$b_4=2.094\,273\,453\,941\,2$	$b_4=-5.104\,720\,900\,166\,2\times10^{-3}$
$t_1=0.477\,915\,973\,567\,38$	$t_2=0.286\,636\,849\,418\,61$

TABLE VIII. Fitted coefficients for potential β.

$a_0 = 9.171\,260\,792\,103\,9$	$a_0 = 4.845\,697\,957\,441\,8 \times 10^{-2}$
$a_3 = 0.327\,587\,552\,644\,87$	$a_3 = 3.278\,322\,768\,358\,1 \times 10^{-2}$
$a_4 = 5.856\,275\,547\,915\,8$	$a_4 = 1.455\,299\,186\,965\,4 \times 10^{-4}$
$a_5 = 403$	$a_5 = -6.218\,944\,811\,030\,8 \times 10^{-2}$
$b_0 = -3.068\,181\,597\,764\,4$	$b_0 = 1.126\,428\,485\,396\,0 \times 10^{-2}$
$b_3 = -1.913\,901\,009\,435\,2$	$b_3 = 1.438\,327\,669\,086\,4 \times 10^{-3}$
$b_4 = 1.263\,933\,651\,815\,4$	$b_4 = -1.018\,165\,605\,647\,6 \times 10^{-2}$
$b_5 = 7.354\,614\,232\,295\,1\ 10^{-2}$	$b_5 = -3.556\,988\,817\,812\,1 \times 10^{-4}$
$t_1 = 0.477\,915\,973\,567\,38$	$t_2 = 0.286\,636\,849\,418\,61$

dle points m and M of type (3,0) and type (2,1), respectively. The meaning of the shaded symbols is given in the caption. Note that the eigenvalue relative to the z direction is always positive and that because of its symmetry the saddle point E always has two identical values.

An alternative way of describing the shape of the derived potentials is with figures showing the isoenergy curves drawn on the plane of isosceles triangles (embedded in the configuration space). In this description (see, for example, Fig. 2), the x axis represents the radius in configuration space, and the y axis represents the coordinate s_2. Hence, y represents the geometry of the configuration (equivalent to knowing the angles in the isosceles triangle), and x represents the extension of the configuration. The various geometries can be seen as follows: $y = 1$ (top of the figure), degenerate isosceles triangles (configuration $D_{\infty h}$: the three atoms are aligned); $y > 0$, obtuse isosceles triangles; $y = 0$, equilateral triangles; $y < 0$, acute isosceles triangles; $y = -1$ (bottom of the figure), degenerate isosceles triangles (two atoms at the same location).

Figures 2–6 illustrate the bottom of the energy surfaces so as to emphasize the order of the first saddle points. The white areas in Figs. 2, 3, and 5 represent low energies, and the dark areas represent high energies. Figures 4 and 6 illustrate the total isoenergy curves of potentials α and β, and are concentric around the energy minimum. The only critical point omitted in this description is the global maximum which is the origin ($x = 0$, not represented). Note in Fig. 4 the appearance of a first saddle point close in space and energy to the equilateral saddle point. Two additional saddle points (obtained through atomic permutations) surround the equilateral point, and this results in a large increase in free volume above this point. This may significantly increase the probability of finding the system above the first saddle point and therefore affect the hopping frequency between the three minima in the total energy. Figure 6 illustrates a more desirable topology. The equilateral saddle point is actually a local minimum although too shallow to be seen in the figure. The maximum increase in energy away from the equilateral saddle point along the $+y$ direction is less than 5×10^{-3} eV.

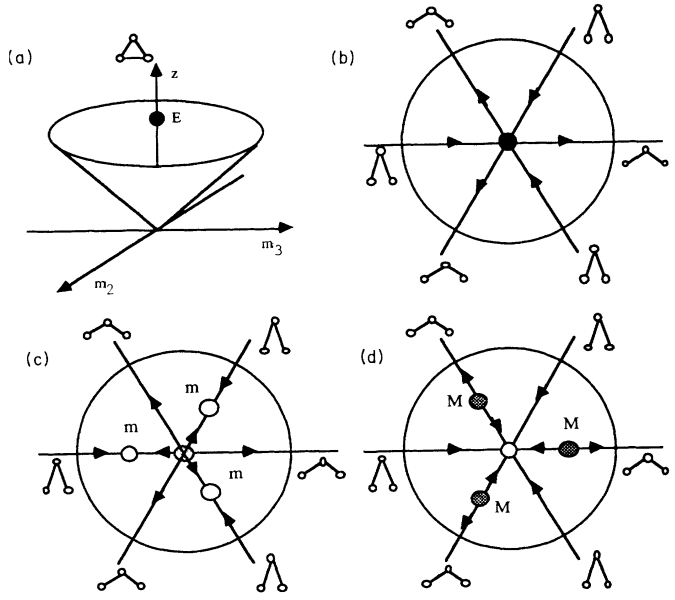

FIG. 1. Possible morphologies which approximate the three-body energy surface around the equilateral saddle point (denoted E). The symbols are ●, degenerate saddle point: Two eigenvalues are equal to zero; the other one is positive. ○, type (3,0): Three eigenvalues are positive; it is a minimum. ● , type (2,1): Two eigenvalues are positive; one is negative. ⊗ , type (1,2): One eigenvalue is positive, two are negative.

III. APPLYING THE TWO- AND THREE-BODY DESCRIPTION TO BULK SILICON

A. Basis for an N-body expansion

The N-body expansion for the total energy of bulk silicon is poorly understood. It is obvious, for reasons of convergence, that the magnitude of each term should decrease with its increasing order in the expansion. There is however, no definitive information on the rate with

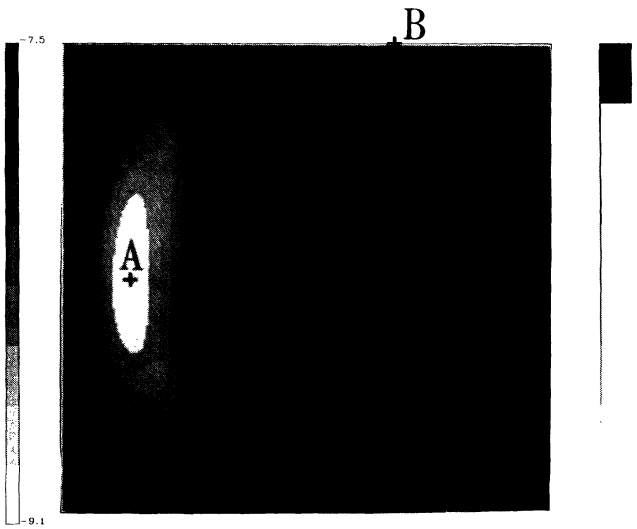

FIG. 2. Two-body contribution, used with potentials α and β. Note the presence of a deep minimum for an equilateral configuration (A) and a saddle point for a $D_{\infty h}$ configuration (B).

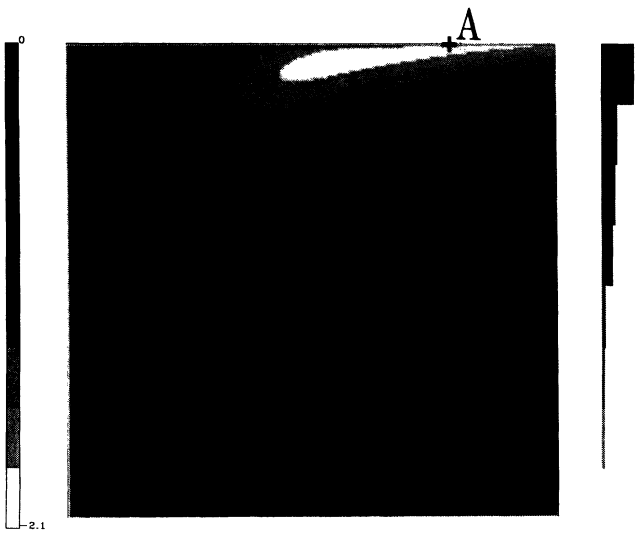

FIG. 3 Three-body contribution; potential α. Note the presence of a minimum for a $D_{\infty h}$ configuration (A), a first saddle point for an acute isosceles configuration (B), and a second nondegenerate saddle point for an equilateral configuration (C).

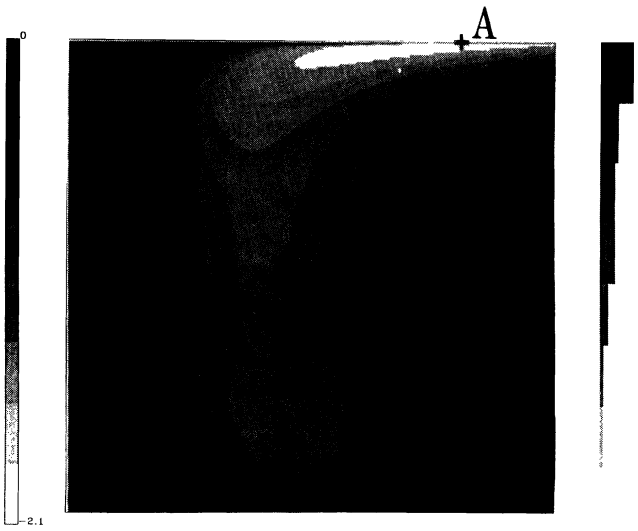

FIG. 5. Three-body contribution, potential β. Note the presence of a minimum for a $D_{\infty h}$ configuration (A) and a single degenerate saddle point for an equilateral configuration (B).

which this magnitude decays, or on the values taken by the first terms in the expansion. It would therefore seem possible to assume that the convergence is fast enough to consider the terms neglected in the expansion (fifth order and above) as a perturbation (the meaning of which is clarified below) of the terms that are retained, and then subsequently check the validity of this hypothesis. Having stated this assumption, it is soon apparent that the overall contribution of the neglected terms is not small and that their effects must be taken into account through a screening of the terms of lower order. Yet, from the morphological point of view (which is of current interest), the neglected terms would be considered as a small perturbation if they did not change the topology given by the first terms of the expansion. This leads to the following hypothesis upon which subsequent discussion is based: *Despite their non-negligible contribution to the total energy, the terms of order higher than 4 in an N-body expansion do not perturb the topology dictated by the first terms of the expansion.*

The principal reason for believing that this is true is the following. The number of p-body terms to be considered increases rapidly with p. Hence, the magnitude of each term will be that much smaller as p increases. After summation over the various p-body configurations,

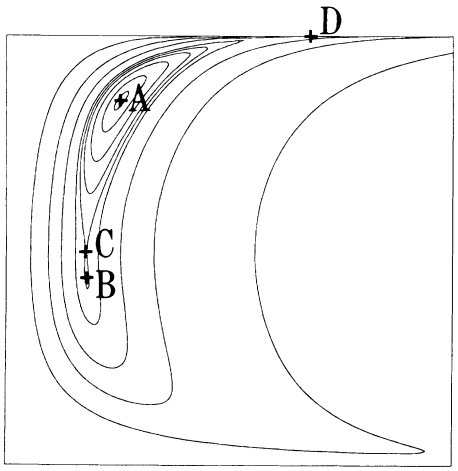

FIG. 4. Total energy, potential α, case of overcompensation. Note the presence of a minimum for an obtuse configuration (A) (intermediate between the equilateral minimum of the two-body term and the $D_{\infty h}$ minimum of the three-body term), a first saddle point for an acute isosceles configuration (B), a second nondegenerate saddle point for an equilateral configuration (C), and a third saddle point for a $D_{\infty h}$ configuration (D) (saddle points are ordered according to their energies).

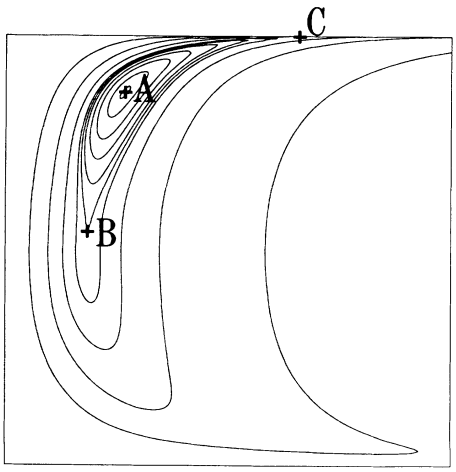

FIG. 6. Total energy, potential β, case of undercompensation. Note the presence of a minimum for an obtuse configuration (A), a first degenerate saddle point for an equilateral configuration (B), and a second saddle point for a $D_{\infty h}$ configuration (C).

an averaging of the shape is expected, resulting in a flat contribution.

It is then a natural step in this approach to use the "exact" two- and three-body terms of the N-body expansion computed in Sec. II. The potentials thus obtained would determine the basic features of the N-body potential topology. The four-body term can then be chosen so as to account for all the remaining terms in the expansion. Since the process of exploring the four-body configuration space is too demanding (it is six dimensional), the morphology of the four-body potential is chosen and the properties of bulk silicon are obtained by means of parametric adjustment. In this process, the potential is subject to limited deformations that preserve the chosen morphology.

The special appeal of this approach lies in the fact that the screening of the neglected terms is only taken into account in the last term retained. The advantages of this method may be listed as follows.

(a) This approach is necessary if construction of a classical potential that correctly describes both small clusters and the bulk is hoped for. Indeed, reproducing the properties of diatomic and triatomic silicon makes it necessary for the two- and three-body parts to be the exact terms.

(b) There are two main differences between a three-body potential and a four-body potential. The first is the fact that when evaluated, for example, on a configuration of four atoms, a four-body potential vanishes if one of the four atoms is far away from the other three. However, this is not necessarily the case for the sum of the three-body potentials. A similar difference exists between the terms of the expansion that are neglected and the terms that are retained. This difference can be interpreted as the existence of asymptotic directions (subspaces) in the barycentric configuration space (configuration space divided by global translations) of p atoms, along which the sum of three-body terms will keep nonzero values, whereas the p-body terms will vanish uniformly far away from the origin (the origin in the barycentric configuration space is the configuration where N atoms are at the same location). More generally, the barycentric p-body configuration space is seen to contain subsets F_q, composed of the configurations where q atoms are at the same location. A sum of q-body terms will then take nonzero values in the neighborhood of F_q, whereas a p-body term will vanish on F_q, provided that the distance to the origin is large enough. It is then noted that the series of these subsets is decreasing, i.e., q greater than r implies that F_q is included in F_r. For this reason, a four-body potential is expected to represent a better approximation of a neglected term than a three-body potential would. This, again, suggests that the screening term should be accounted for in the last term not neglected.

(c) The second difference between a three- and a four-body potential is the way the numbers of three- and four-body terms vary with the number of neighbors of each atom. In principle, each summation of p-body terms should be made over all possible p-uplets contained in the system. In practice, the p-uplets are limited to those contained within the first shells of neighbors of each atom, which is consistent with the physical idea that these potentials have a finite range of interaction. Hence, if n is the number of neighbors taken into account, the number of p-body terms to be considered per atom is equal to

$$\frac{1}{p}C_{p-1}^{n} .$$

The number of neighbors to be considered should be given by the range of interaction of the exact two-body term which is found to become negligible between the third and fourth nearest neighbor in the diamond cubic structure of silicon. The number of neighbors n is therefore equal to 28, resulting in the various numbers of terms per atom given in Table IX.

It is seen that the number of four-body terms varies as n^3, whereas the number of three-body terms varies as n^2, which makes the number of two-body terms relatively more important when n decreases. Since the number of five-body terms, for example, varies as n^4, it seems better to account for the five-body term through a modification of the four-body term, rather than through a modification of the two- or three-body terms. In this way, it may be possible to obtain a better description of the atomic forces, especially in situations where the number of neighbors is perturbed, which is the case near most crystalline defects.

B. Computational results

The computation of the exact first two terms of the N-body expansion shows that the two-body term is large with a long-range interaction (up to the fifth nearest neighbor in the diamond cubic structure). It has a minimum of about -3.0 eV reached at a distance of 2.11 Å and a strongly repulsive short-range behavior. The three-body term is comparatively smoother, being nowhere smaller than -2.0 eV and nowhere larger than 4.0 eV. It gives rise to an even longer range of interaction, inducing correlations with the sixth nearest neighbor of each atom. The contribution of these terms to the calculation of the total energy is as follows: two-body term, -8.85 eV, three-body term, -40.94 eV.

The force constants for the first six nearest neighbors have also been computed. They are represented by the following matrices:[14]

TABLE IX. Number of terms per atom for the four-nearest-neighbor shells.

	Neighbors	Two-body terms	Three-body terms	Four-body terms	Five-body terms
p shells	n	$n/2$	$n(n-1)/6$	$n(n-1)(n-2)/24$	$n(n-1)(n-2)(n-3)/120$
2 shells	16	8	40	140	364
3 shells	28	14	126	819	4095
4 shells	32	16	165	1240	7192

$$\text{first-nearest neighbor } (1,1,1): \begin{bmatrix} \alpha_1 & \beta_1 & \beta_1 \\ \beta_1 & \alpha_1 & \beta_1 \\ \beta_1 & \beta_1 & \alpha_1 \end{bmatrix}, \quad \text{second-nearest neighbor } (2,2,0): \begin{bmatrix} \alpha_2 & \beta_2 & \gamma_2 \\ \beta_2 & \alpha_2 & \gamma_2 \\ -\gamma_2 & -\gamma_2 & \delta_2 \end{bmatrix},$$

$$\text{third-nearest neighbor } (-1,-1,-3): \begin{bmatrix} \alpha_3 & \beta_3 & \gamma_3 \\ \beta_3 & \alpha_3 & \gamma_3 \\ \gamma_3 & \gamma_3 & \delta_3 \end{bmatrix}, \quad \text{fourth-nearest neighbor } (0,0,4): \begin{bmatrix} \alpha_4 & 0 & 0 \\ 0 & \alpha_4 & 0 \\ 0 & 0 & \delta_4 \end{bmatrix},$$

$$\text{fifth-nearest neighbor } (3,3,1): \begin{bmatrix} \alpha_5 & \beta_5 & \gamma_5 \\ \beta_5 & \alpha_5 & \gamma_5 \\ \gamma_5 & \gamma_5 & \delta_5 \end{bmatrix}, \quad \text{sixth-nearest neighbor } (2,2,4): \begin{bmatrix} \alpha_6 & \beta_6 & \gamma_6 \\ \beta_6 & \alpha_6 & \gamma_6 \\ \varepsilon_6 & \varepsilon_6 & \delta_6 \end{bmatrix}.$$

The values obtained for the various elements of these matrices are given in Table X.

From these results it is seen that the sum of the total-energy contributions is negative and one order of magnitude larger than the expected energy for silicon. In addition, the force constants show very strong correlations up to the fourth-nearest neighbor. A four-body term capable of screening this behavior would therefore have to yield a large and positive contribution to the total energy. Furthermore, the requirement that it must screen the long-range interaction of the two- and three-body potentials implies that it itself has a long range of interaction.

In an attempt to circumvent these problems, the four-body term was decomposed into two parts, one being a pure screening term with a long-range interaction and the other being a short-range four-body term, the morphology of which was well controlled. The screening term was chosen to be

TABLE X. Computed elements of the dynamical matrix.

Force constants	LCAO[a] values (Ref. 14)	Two-body contribution	Three-body contribution
a_1	−4.112	−1.505	−12.62
b_1	−2.854	−0.765	−11.97
a_2	−0.098	0.324	2.217
b_2	−0.089	0.521	3.563
g_2	−0.098	0.0	0.389
d_2	0.373	−0.198	−2.080
a_3	−0.0085	−0.0250	−0.435
b_3	−0.0104	0.0485	−0.337
g_3	−0.0075	0.1454	−0.412
d_3	0.0110	0.3627	−1.043
a_4	0.0093	−0.0141	−0.342
d_4	0.0051	0.1350	0.372
a_5	−0.0093	0.0259	0.349
b_5	0.0024	0.0312	0.511
g_5	0.0411	0.0104	0.102
d_5	0.0837	−0.0018	0.092

[a]Linear combination of atomic orbitals.

$$V_s(u_1,u_2,u_3,u_4) = \left[\lambda_2 \sum_{\text{pairs}} V_2 + \lambda_3 \sum_{\text{triplets}} V_3\right] f(x_1), \tag{19}$$

where u_i represents the position of atom i, the summations of V_2 and V_3 are extended over all pairs and triplets contained in the quadruplet of interest, and f is a cutoff function of the four-body configuration-space radius x_1. Using this method, the total energy and lattice parameter of diamond cubic silicon was successfully reproduced. Acceptable force constants were also obtained but the computed (001) surface energy was negative. As pointed out earlier, the number of two-, three-, and four-body terms vary as n, n^2, and n^3, respectively, where n is the number of neighbors. Therefore, since the number of neighbors of each atom decreases close to the surface, the number of two-body terms becomes relatively more important than the number of three-body terms, and so does the number of three-body terms with respect to the number of four-body terms. This implies that the positive contribution to the total energy of the four-body terms cannot, in these circumstances, compensate for the negative contribution of the two- and three-body terms. This explains the resulting negative surface energy. A solution to this problem would be to shorten the range of interaction of the four-body term. The number of four-body terms would then be constant almost up to the surface, in contrast to the numbers of two- and three-body terms which begin to decrease much earlier. Unfortunately, the need to screen the long-range interactions of the two- and three-body terms makes this approach intractable, because then a long-range four-body term becomes necessary.

It is clear that the above results strongly indicate (though do not prove) that the original hypothesis stated above is incorrect and that the terms of order higher than 4 do perturb the global topology dictated by the exact two- and three-body terms. To examine this further, a different and final approach was attempted to try and account for the terms neglected in the truncated expansion. Instead of retaining the exact two- and three-body terms and accounting for the screening with a four-body term, the total energy is determined only by the two- and

three-body terms which are screened directly. However, in this approach the topology of both the two- and the three-body terms is preserved such that the energy is given by the following, using four fitting parameters:

$$E=\lambda_1\sum_{i,j}V_2(\lambda_2 r_i,\lambda_2 r_j)+\lambda_3\sum_{i,j,k}V_3(\lambda_4 r_i,\lambda_4 r_j,\lambda_4 r_k)\ . \quad (20)$$

Using this formalism, however, it was found that the diamond cubic structure was not the global-energy minimum. The best parametric choices favored close-packed structures (fcc, for example), so that the inclusion of a four-body term is still necessary if this topology of the two- and three-body terms is to be retained.

IV. CONCLUSIONS

In the first part of this paper a study of the Born-Oppenheimer surface for three silicon atoms was presented. For triatomic clusters, the three-body expansion for the total energy can be expressed and computed precisely using first-principles pseudopotentials. Preliminary understanding of the three-body configuration space and that of the equilateral saddle point led to the surprising conclusion that the Born-Oppenheimer surface for three atoms is not likely to be generic (one of its saddle points is likely to be degenerate). Intuitively, this may be understood as follows. The total energy of three atoms should increase during a deformation from the equilateral saddle point towards an acute isosceles configuration, and subsequently decrease during a deformation towards an obtuse isosceles configuration. This behavior implies that the second differential of the total energy at this saddle point is degenerate. It is therefore impossible, in general, to choose two- and three-body potentials that will produce this behavior. The model potentials (α and β) that were constructed show slightly different topologies which may affect the dynamics of the cluster. The best potential in this respect was found to be potential β, which should, in fact, represent an excellent approximation for the Born-Oppenheimer surface of three silicon atoms.

Because it was not possible to model terms of order 5 the N-body expansion for the crystal was truncated at order 4. It was then assumed that the remaining terms did not perturb the topology dictated by the first terms and that their effect could be well represented in the four-body term. An accurate modeling of the exact first two terms of the N-body expansion showed that their contribution to the total energy of the crystal and to the force constants was too large by an order of magnitude and induced a very long range of interaction. These characteristics led to the construction of a four-body term with a relatively large amplitude and range of interaction. These resulting features of the global potential for the crystal proved to be incompatible with obtaining a positive surface energy and invalidated the initial hypothesis. It was therefore concluded that successful application of the N-body expansion in the case of bulk silicon would require knowledge of terms of order higher than 4, which is presently difficult to obtain. Another method was attempted which involved a rescaling of the two- and three-body terms such that their morphology was preserved. The resulting potentials proved incapable of giving the correct equilibrium structure. It is possible that this situation could be improved by the use of an additional four-body term, but this was not attempted in the present study.

Finally, the present study of the Born-Oppenheimer surface of triatomic silicon shows that the terms of the N-body expansion are strongly dependent on one another. This remark is of profound significance, since it implies that the morphology of the Born-Oppenheimer surface of N atoms may show unexpected nongeneric characteristics which would then preclude any analyses in terms of generic local potentials.

ACKNOWLEDGMENTS

The authors are grateful to Professors J. D. Joannopoulos, R. W. Balluffi, and R. Macpherson for their critical review of this work. Support by the French Délégation Générale pour l'Armement (P.D.) and the U.S. Department of Energy (Grant No. DE-FG-02-8ER-45310) (P.D.B.) is also gratefully acknowledged. Supercomputer time was provided by the National Science Foundation at the Pittsburgh Supercomputer Center.

*Present address: Service Physique Atomique et Plasmas, Centre d'Etude de Limeil Valenton, BP 27, 94190 Villeneuve Saint-Georges, France.

[1]J. D. Joannopoulos, in *Physics of Disordered Materials,* edited by D. Adler, H. Fritzsche, and S. R. Orshinsky (Plenum, New York, 1985), p. 19.

[2]A. T. Paxton, A. P. Sutton, and C. M. M. Nex, J. Phys. C **20**, L263 (1987).

[3]F. H. Stillinger and T. A. Weber, Phys. Rev. B **31**, 5262 (1985).

[4]K. Raghavachari and V. Logovinsky, Phys. Rev. Lett. **55**, 2853 (1985).

[5]G. Pacchioni and J. Koutecky, J. Chem. Phys. **84**, 3301 (1986).

[6]K. Balasubramanian, Chem. Phys. **135**, 283 (1987).

[7]P. Dallot, P. D. Bristowe, and M. Demazure, preceding paper, Phys. Rev. B **46**, 2133 (1992).

[8]M. L. Cohen and V. Heine, in *Solid State Physics,* edited by H. Ehrenreich, F. Seitz, and D. Turnbull (Academic, New York, 1970), Vol. 24, p. 37.

[9]M. C. Payne, M. P. Teter, D. C. Allen, and J. D. Joannopoulos (unpublished).

[10]R. Car and M. Parrinello, Phys. Rev. Lett. **55**, 2471 (1985).

[11]P. Hohenberg and W. Kohn, Phys. Rev. **136**, B864 (1964).

[12]D. R. Hamann, M. Schlüter, and C. Chiang, Phys. Rev. Lett. **43**, 1494 (1979).

[13]*Handbook of Chemistry and Physics,* 68th ed., edited by R. C. Weast (CRC Press, Boca Raton, FL, 1988).

[14]A. Mazur and J. Pollman, Phys. Rev. B **39**, 5261 (1989).

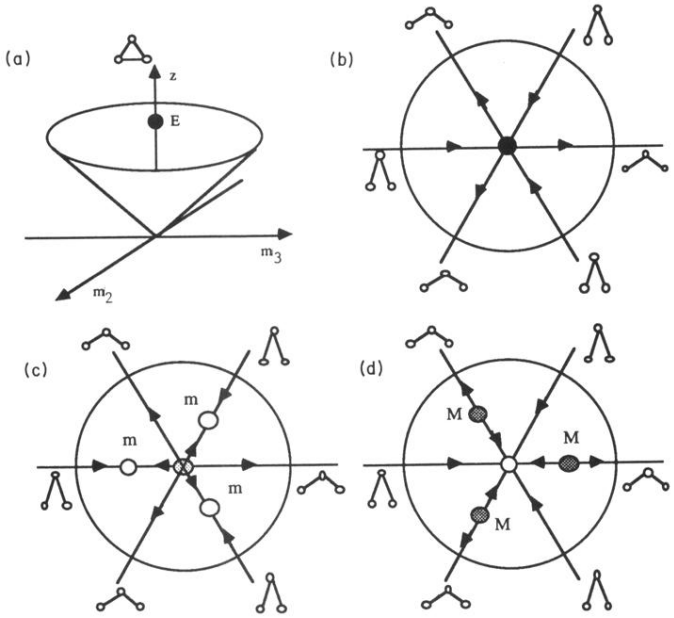

FIG. 1. Possible morphologies which approximate the three-body energy surface around the equilateral saddle point (denoted E). The symbols are ●, degenerate saddle point: Two eigenvalues are equal to zero; the other one is positive. ○, type (3,0): Three eigenvalues are positive; it is a minimum. ◉ , type (2,1): Two eigenvalues are positive; one is negative. ⊗ , type (1,2): One eigenvalue is positive, two are negative.

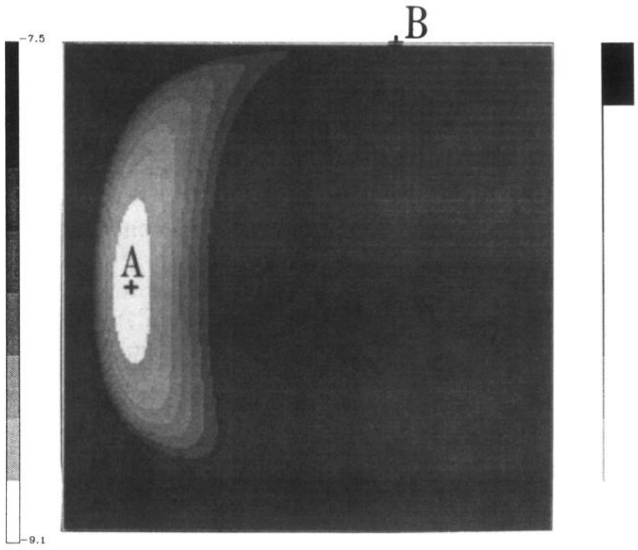

FIG. 2. Two-body contribution, used with potentials α and β. Note the presence of a deep minimum for an equilateral configuration (A) and a saddle point for a $D_{\infty h}$ configuration (B).

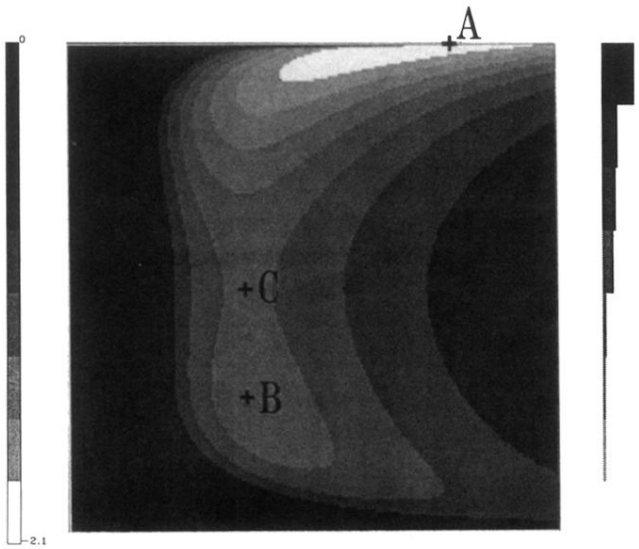

FIG. 3 Three-body contribution; potential α. Note the presence of a minimum for a $D_{\infty h}$ configuration (A), a first saddle point for an acute isosceles configuration (B), and a second nondegenerate saddle point for an equilateral configuration (C).

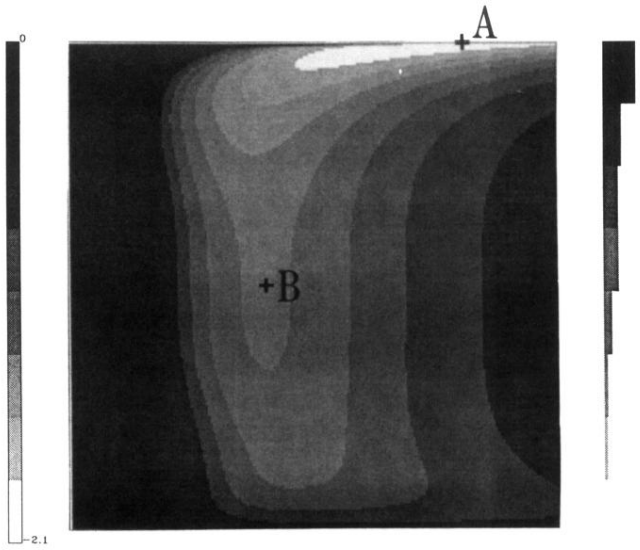

FIG. 5. Three-body contribution, potential β. Note the presence of a minimum for a $D_{\infty h}$ configuration (A) and a single degenerate saddle point for an equilateral configuration (B).